AIAA 2001-2121

Full-Scale Numerical Model of a Rijke-Type Pulse Combustor

Joseph Majdalani
Marquette University
Milwaukee, WI 53233

B. Entezam and W. K. Van Moorhem
University of Utah
Salt Lake City, UT 84112

7th AIAA/CEAS Aeroacoustics Conference
28–30 May 2001
Maastricht, The Netherlands

Full-Scale Numerical Model of a Rijke-Type Pulse Combustor

J. Majdalani*
Marquette University, Milwaukee, WI 53233
and
B. Entezam† and W. K. Van Moorhem‡
University of Utah, Salt Lake City, UT 84112

In this paper a numerical model is developed to investigate the thermoacoustic conversion of heat into sound inside a Rijke tube. This study is carried out in an attempt to better understand the internal coupling between heat addition, pressure and velocity oscillations inside pulse combustors. In fact, similar coupling is believed to exist in other combustion devices including rocket motors at the verge of instability. In light of the recent progress in computational fluid dynamics (CFD), it is now possible to model quite effectively the compressibility effects bridging the gap between thermal and pressure oscillations. Our CFD results have been favorable in that they concurred with experimental observations. Self-sustained thermal oscillations near the heat source are found to be responsible for driving the acoustic pressure excitation. When acoustic velocity and pressure have maximum additive amplitudes, an optimal conversion of thermal energy into mechanical energy occurs. The latter is manifested in the form of acoustic intensity, which is the product of acoustic velocity and pressure. Below a threshold value in power input to the internal heat source, no self-sustained acoustic oscillations have been observed. Conversely, when a critical power input to the heater is exceeded, resonance is triggered in the form of pronounced acoustic amplification. The acoustic pressure and velocity mode shapes concur with classic theory except near the heater source where a local increase in the velocity amplitude is noted. During limit-cycle oscillations, the acoustic pressure is found to lead thermal fluctuations by a 45 degree angle. This result may be used to specify the phase angle in Carvalho's analytical formulation which predicted a value under 90 degrees. Overall, numerical results indicate a strong pressure dependence on heat fluctuations. In fact, the modulus of thermal oscillations is found to be directly proportional to the modular product of acoustic velocity and pressure. In relation to solid and hybrid rocket motors, they predict a strong thermoacoustic, noise generating coupling in the forward half of the motor.

Nomenclature

a_0	= mean speed of sound inside the Rijke tube
A	= oscillatory pressure amplitude
C_p	= constant pressure specific heat
l	= internal tube length
m	= oscillation mode, $m = 1,2,3,...,\infty$
p'	= oscillatory pressure component
Q	= heat energy
q	= heat transfer rate, dQ/dt
q'	= oscillatory heat transfer rate
T	= temperature
t	= time
u'	= oscillatory velocity component
x	= axial distance measured from the bottom
γ	= mean ratio of specific heats
ρ	= air density
ω	= circular frequency, $m\pi a_0 / l$

Subscripts

0	= mean value
obs	= obstacle or heat source
∞	= surrounding mean flow condition

*Assistant Professor, Department of Mechanical and Industrial Engineering. Member AIAA.

†Research Scientist, Datum Corp., Irvine, CA. Member AIAA.

‡Professor, Department of Mechanical Engineering. Senior Member AIAA.

I. Introduction

CONSIDER an open-ended circular tube standing vertically. Placing a heat source at some short distance from the bottom produces large sound pressure levels that are audible a large distance away. This phenomenon can occur inside the thermoacoustic pipe known as the Rijke tube. Inside this device, the mechanisms leading to the implicit conversion of heat fluctuations into acoustic energy has fascinated scientists for many years now. Due to its relevance to a number of practical applications, Rijke tube studies have received much scrutiny in the past.[1-16] Despite the amount of attention given to this and other types of pulse combustors, previous investigations have been limited to either theoretical or experimental investigations. In order to supplement the only apparent numerical study by Raun and Beckstead,[12] the current article will be devoted to a comprehensive computational verification of the Rijke's thermofluid character. To that effect, the increased computational power available today will be exploited to develop a two-dimensional compressible flow model that is capable of coupling both thermal and fluid flow components of the problem. Our main interest is to determine how accurate numerical simulations can be, if at all possible, in reproducing the phenomena observed in the Rijke tube. Due to the absence of previous full-scale computational models, another goal is to determine the key mathematical equations that may be necessary to achieve a reasonable solution. Aside from the scientific merit associated with achieving a numerical verification, the results are hoped to help construct a valid thermoacoustic model starting from the fundamental conservation equations.

Another motivation for this numerical study is the increased freedom and flexibility in varying the problem's physical parameters. In view of wider range numerical experiments that are now possible, we hope to gain added insight into the physics underlying the thermoacoustic phenomena in pulse combustors.

To set the stage, the present analysis begins by a brief classification of three types of pulse combustors. This is followed by a description of the self-excited oscillator that defines the character of the Rijke tube. Next, the main ingredients of the computational model are explained. Forthwith, results are presented and shown to concur with existing experimental and theoretical predictions. In addition to providing an independent verification, results are shown to be useful in clarifying existing speculations. As a windfall, they seem to provide solutions to some unresolved terms arising in former analytical models.

II. Classification

The classic pulse combustors[17,18] can be subdivided into three categories depending on their operational system configuration. The first is a closed-open, quarter-wave instrument known as the Schmidt tube. The second is the Helmholtz resonator, involving either a closed-open or an open-open system. The third is the Rijke tube, which is an open-open, half-wave system.

The Schmidt tube is the predecessor of the German V-1 rocket motor. It comprises three sections: the inlet, the combustion chamber, and the tail or exhaust pipe. The inlet section consists of one-way valves which open or close depending on whether the combustor pressure is lower or higher than the pressure upstream of the valves.

The Helmholtz resonator[19] consists of a rigid-wall cavity which has at least one short and narrow neck through which the enclosed fluid can communicate with the external medium.

The Rijke tube falls into the third type of pulse combustors. It denotes a vertical tube that comprises a single heat source and two isobaric ends.

A. The Rijke Tube

The earliest accounts of thermoacoustic oscillations can be traced back to Rijke[20] in 1859. In his work, Rijke reported that strong oscillations could occur when a heated wire screen was placed in the lower half of an open-ended vertical pipe (see Fig. 1). These acoustic oscillations were found to stop altogether when the top end of the pipe was sealed. This indicated that upward convective air currents in the pipe were essential for thermoacoustically driven oscillations to take place. As could be inferred from Fig. 1, the Rijke tube is a half wave pulse combustor with an acoustic wavelength that is actually twice the length of the tube. Based on laboratory observations, oscillations reached maximum amplification when the heater was centered in the bottom half. At that location, both acoustic pressure and velocity amplitudes are additive. For heater positions in the upper half of the pipe, damping instead of driving occurred. Rijke believed that rising convection currents expanded in the region of the heated screen and compressed downstream from the heater due to cooling at the pipe walls. These successive expansions and contractions were blamed for the intense production of sound. The foregoing explanation was useful but limited in that it could not address the details of heat exchange mechanisms causing the actual oscillations.

Since Rijke's landmark investigation, there have been several attempts to explain this phenomenon.[1,3-9,11,13,14,21-30] In fact, Lord Rayleigh[20] has proposed, shortly thereafter, a criterion in which he addresses the relationship between heat addition and sound waves.

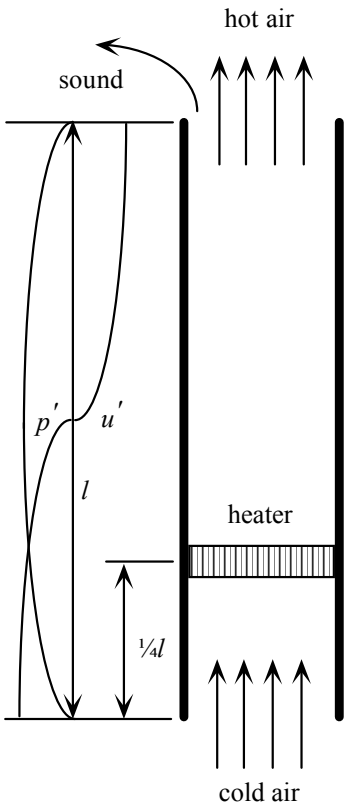

Fig. 1 The Rijke tube and associated fundamental acoustic wave structure.

According to Rayleigh, acoustic excitation or attenuation may occur depending on whether heat is added to a sound wave at the high or low temperature phases of its cycle. Furthermore, since compression in a sound wave is adiabatic, pressure and temperature fluctuations are in phase. As a result, heat addition during a positive pressure disturbance phase (leading to an upward wave) corresponds to a high temperature phase and, thereby, has potential to trigger acoustic excitation. Clearly, an opposite effect is to be expected when the pressure disturbance phase is negative, corresponding to a downward wave. Rayleigh's criterion gives a different perspective for explaining the sound generated inside pulse combustors.

In the Rijke tube, for example, the grid (gauze, or heat source) heats the surrounding air and causes it to rise. Acoustically induced particle displacements are superimposed on the naturally convected flow. When acoustic particle displacements are positive upward, fresh cold air crosses the heated grid, but when negative, hot air from above is filtered through. During the upward pass, maximum heat transfer occurs between the heat source and the air due to the large temperature differential with the cooler air. Since the timing in the acoustic cycle is such that maximum heat transfer corresponds to a positive particle displacement (with favorable, upward motion), an ideal situation is created to promote acoustic wave growth.

If the grid is now placed in the upper half of the pipe, acoustic velocity and pressure exhibit unfavorable phases. Pressure acts adversely, in a direction that opposes particle motion. Under such conditions, acoustic amplification is suppressed. If the phase between pressure and heat release rate is favorable, acoustic amplitudes are additive, disturbances gain energy, grow in magnitude, and may lead to undesirable structural implications. A similar mechanism is associated with the so-called 'reheat buzz,' a common jet engine instability of the reheat system. In the jet engine, however, buzz is triggered by fluctuations in the combustion rate. These fluctuations, in turn, are caused by acoustic velocity oscillations disturbing the reheat afterburner flame.

B. The Self-excited Oscillator

For the Rijke tube, the wave equation can be written with the heat addition term acting as a driving function. When this is accomplished, the following governing expressions are obtained for both acoustic pressure and velocity[31]

$$\frac{1}{a_0^2}\frac{\partial^2 p'}{\partial t^2} - \nabla^2 p' = \frac{1}{C_p T_0}\frac{\partial q'}{\partial t} \tag{1}$$

$$\frac{\partial^2 u'}{\partial t^2} - a_0^2\,\nabla^2 u' = \frac{1-\gamma}{\rho_0}\frac{\partial q'}{\partial x} \tag{2}$$

Equations (1) and (2) denote the Rijke-tube's self-excited character owing to the nature of the right-hand-side terms. Self-excited oscillations are rather unique due to the preponderance of physical problems that belong to the free or forced types.

In a self-excited oscillator, the energy associated with motion is supplied by an time-dependent quantity that is modulated by the oscillator itself. This quantity can be a force, an electric current, or a heat source, depending on the case at hand. Since the unsteady driving term q' that appears in Eqs. (1–2) is induced by fluctuations in other thermodynamic quantities within the system, the Rijke tube is of the self-excited type. Other familiar examples include mechanical clocks, electronic oscillators, musical wind instruments, bowed string instruments, and the human voice. In these applications, the sustaining force is tied to the alternating motion and cannot persist when the induced motion is suppressed. This explains the subtleties needed to implement a full-scale numerical model. In order for the model to be accurate, it must be able to track the transient behavior and interdependencies of all components and processes involved. Here, when the disturbances generated inside the Rijke tube are fed

back to the existing system energy, the process itself becomes a driving force. Such feedback controls the system's transient response and determines whether acoustic amplitudes will grow or decay. As could be seen via Eqs. (1–2), in order to seek analytical solutions to the problem, the functional form of q' needs to be established. Furthermore, conditions controlling the flowfield on both sides of the heat source must be carefully posited. Determination of q' and its relation to p' and u' is hence desirable. Due to the absence of closed-form expressions linking p', u', and q', one of our goals will be to provide a physical explanation of the pertinent coupling based on the forthcoming numerical experiments.

III. The Computational Model

The Rijke tube is modeled as a pipe that is 90 centimeters in length and 5 centimeters in diameter. The pipe is placed inside a large rectangular enclosure representing a laboratory space. Since the pipe is a body of revolution, all material properties, boundary conditions and flow variables are symmetric with respect to the pipe's centerline. Only one cross-section of the pipe is modeled, thus taking advantage of prevalent symmetry. Figure 2 gives a three-dimensional rendering of the Rijke tube that we modeled as a hollow cylinder inside a room. The computational mesh in the $r-x$ directions is illustrated in Fig. 3. The domain comprises half of the Rijke tube and surrounding space. The ambient atmospheric conditions, including pressure, temperature and density, are used to define the initial conditions at the pipe's inlets and outlets and inside the box representing the room.

The key component of the Rijke tube is this. In order to introduce an actual heat source, a horizontal porous obstacle with a diameter of 3.75 cm is inserted into the tube at a distance of 22.5 cm (i.e., $\frac{1}{4}l$) from the bottom. Thermostatic properties of steel are assigned to the obstacle whose surface porosity is set to correspond to a 90% open area fraction. Inside the obstacle, heat is released gradually from zero to its final value in order to mimic practical heat sources.

A. Numerical Strategy

The numerical procedure involves two successive and equally important stages. The first stage is transient-like, and carries the problem from an initial state of rest to a time of 20 seconds. After the first 20 seconds, the problem would have reached a terminal or limit-cycle condition. Within numerical uncertainty, the terminal or quasi 'steady-state' oscillations exhibit constant amplitudes.

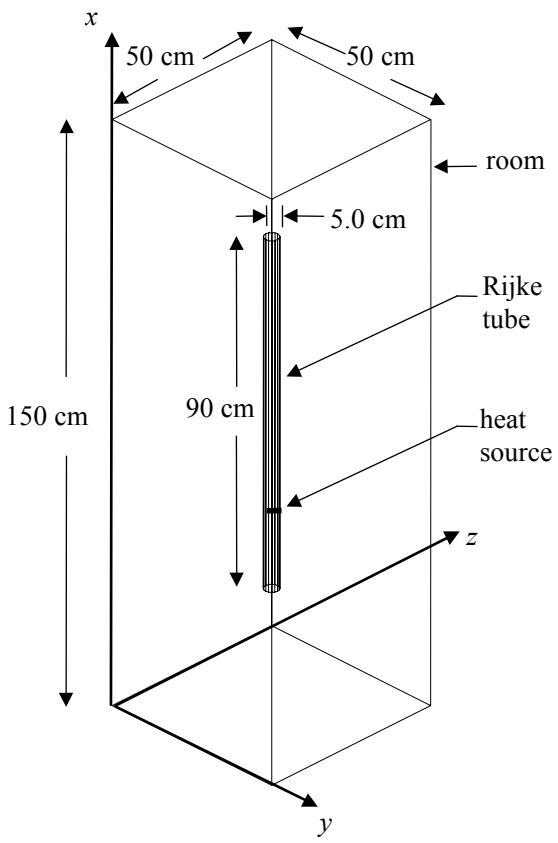

Fig. 2 Three-dimensional representation of the Rijke tube inside a room.

The second stage carries the problem from 20 to 20.025 seconds using a much smaller time step. The increased time resolution is necessitated by the need to track minute temporal changes in the acoustic waves. Throughout the tube, virtual probes are placed at several locations in order to monitor pressures, temperatures, densities and velocities. Our primary input variables are summarized in Table 1. This information is fed into the preprocessor of a commercially available software program (Flow-3D).[32] The latter is utilized with its full compressible flow options and heat transfer subroutines.

IV. Results and Discussion

A number of parametric studies are carried out in an attempt to characterize the internal flow field. A benchmark case is first selected with typical physical dimensions and thermodynamic properties. The acoustic character is analyzed and compared with both experimental and theoretical predictions. After setting up the proper boundary conditions, the temporal evolution of mean and acoustic variables are determined. The location and power supply to the heater source are varied separately in order to assess

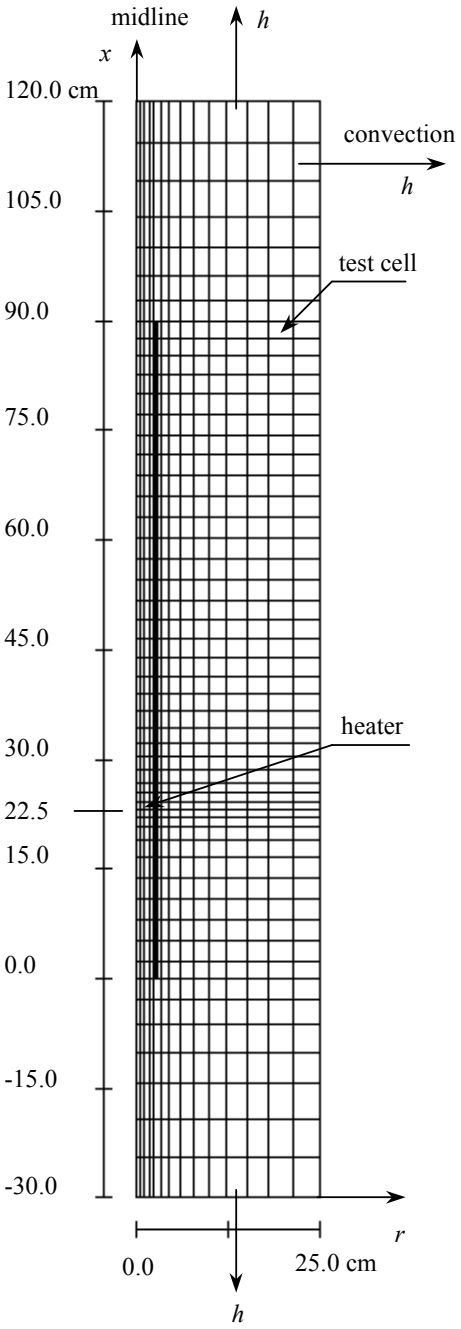

Fig. 3 Computational mesh.

their influence on the solution. Whenever possible, the coupling between thermal and acoustic variables is described.

A. Benchmark Case

In order to set a benchmark, a standard case is defined whose properties correspond to a typical Rijke tube size, gas properties, and heat source power input. As posted in Table 1, our benchmark case is a standard

Table 2. Standard input properties

Pipe	Unit	Input
Material	-	Steel
Diameter	cm	5
Length	cm	5
Wall thickness	cm	5
Thermal conductivity	W/m/K	36
Density-heat capacity Product	$J/m^3/K$	$3.77x10^6$
Heat transfer coefficient	$W/m^2/K$	Calculated
Initial temperature	K	293.0
Obstacle (Heat Source)		
Material	---	Steel
Diameter	cm	3.75
Thickness	cm	1
Location from bottom	cm	22.5
Porosity	---	0.9
Power input	W	430
Thermal conductivity	W/m/K	36
Density-heat capacity Product	$J/m^3/K$	$3.77x10^6$
Heat transfer coefficient	$W/m^2/K$	Calculated
Initial temperature	K	293.0
Gas		
Gas medium	---	Air
Gas constant	J/Kg/K	287
Dynamic viscosity	Kg/m/s	$1.824x10^{-5}$
Specific heat	J/Kg/K	718
Thermal conductivity	W/m/K	0.0251
Initial temperature	K	293.0

run that involves a steady heat release of 430 watts at an optimal heat source position of $\frac{1}{4}l$ from the bottom. Results are summarized in Figs. 4–6.

In Fig. 4, temporal plots are shown, during the first 20 seconds, for pressure, axial velocity, temperature, density and heat transferred to the air. Note that, after about 8.5 seconds, heat, pressure, and velocity oscillations begin. This threshold coincides with the time when the air temperature around the source begins to approach its terminal condition. This condition may be inferred from the leveling out of the temperature curve in Fig. 4. In that region, small temperature oscillations occur but are too small to be discerned without scale magnification (see Fig. 5). As the temperature of the air increases, both pressure and velocities increase as well. This is accompanied by a decline in density as the heated gas expands. Since no acoustic pressure growth occurs prior to the temperature reaching its limit-cycle oscillations, it may be inferred that thermal fluctuations at the heater

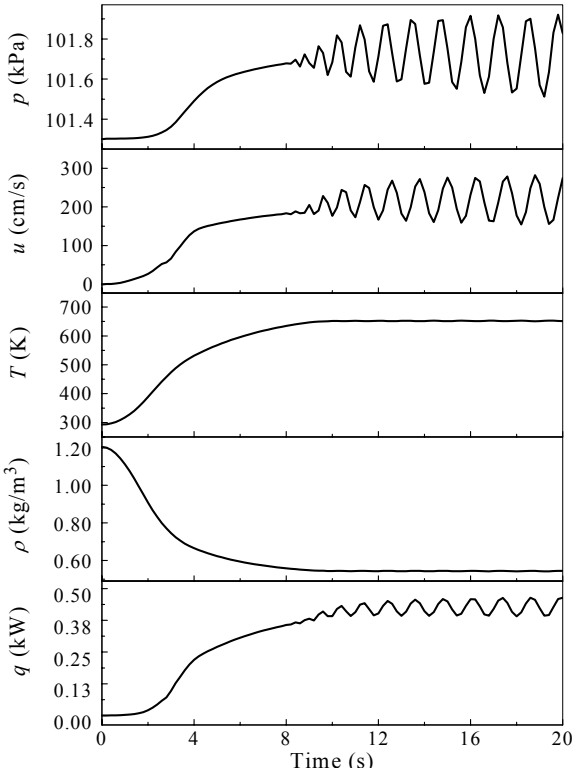

Fig. 4 Time evolution of pressure, axial velocity, temperature, density, and heat transfer during the first 20.0 seconds of the numerical simulations (Stage I). This case corresponds to a power input of 430 watts supplied to a heat source at $x = \frac{1}{4}l$.

location are the main driving factor in producing the acoustic excitation. In a sense, the Rijke tube may be likened to a thermoacoustic pump in which the pumping-like temperature oscillations raise the acoustic energy to substantial audible levels.

The physics underlying these observations may be attributed to the following. As the source temperature begins to rise, a temperature difference between the source and surrounding air is created on both sides of the obstacle surface. The reduced density of the surrounding air causes it to stratify. Natural convection currents are hence produced due to buoyancy. As the heated air rises, it crosses the porous obstacle. The heat transferred from the source to the surrounding air can be determined to be a function of source temperature, ambient air temperature, source area, and average convection heat transfer coefficient. Since all properties are intimately related, the slightest disturbance in a given quantity is echoed in the signals obtained from the remaining variables. The acoustically driven motion is hence established once temperature oscillations become self-sustained.

Figure 5 displays temporal plots of pressure, axial velocity, temperature, density and heat transferred to the air for the limit-cycle oscillation stage (20 to 20.025 seconds). Here, a smaller time step is utilized to track the acoustic growth more effectively. Clearly, Fig. 5 indicates that periodic oscillations are present in all flow variables at a frequency of about 200 Hz. This reassuring frequency matches very closely the acoustically prescribed natural frequency, $f = ma_0/(2l)$, for the fundamental oscillation mode $(m = 1)$ in a pipe with isobaric ends.

B. The Tube's Finite Length

In order to capture the acoustic mode shapes due to the pipe's finite body length, Fig. 6 is used to illustrate the pressure and axial velocity oscillations at several different locations along the pipe. An examination of Fig. 6 suggests that pressure oscillations reach their maxima at the center of the pipe and are small near both ends. Also, pressure oscillations appear to be in phase at any axial location, as one may expect from acoustic wave theory. The velocity plot, on the other hand, shows that velocity oscillations reach their maxima near both ends and are near zero at the center of the pipe. As such, velocity oscillations are 180° out of phase in the lower and upper half-domains. These results exhibit the expected patterns predicted by acoustic theory, thus

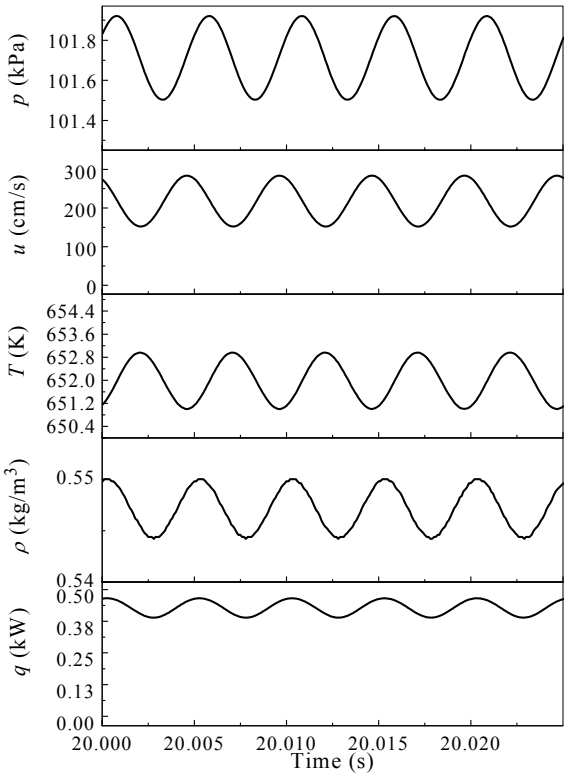

Fig. 5 As in the previous figure, we plot the time evolutions of the principal variables during limit-cycle oscillations (Stage II). Here the time step is reduced to 0.0025 s.

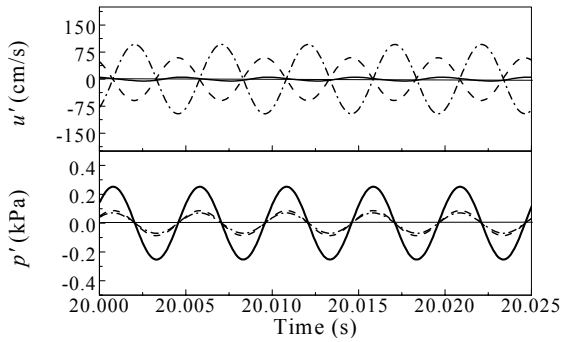

Fig. 6 Acoustic pressure and axial velocity shown at three key locations corresponding to $x = \frac{1}{2}l$

eliminating the possibility of being the mere outcome of computational error. Moreover, these trends appear to be in agreement with experimental observations in Rijke tubes.[1,4,5,7,16]

C. Proper Boundary Conditions

One advantage of numerical experiments is that they can help define a complete mathematical model with valid auxiliary conditions. This may be accomplished by verifying the types of boundary conditions that are necessary for a successful assault on the problem. In our case, pressure, temperature and density distributions had to be carefully selected at key locations for $t < 0$. Subsequently, from $t = 0$ until the oscillations began, the evolution of the primary thermodynamic variables had to be tracked numerically along the length of the tube. Results obtained are shown in Fig. 7 for the three principal variables. Note, in particular, the temporal solution across the heat source where abrupt changes take place. Prior to the inception of thermoacoustic oscillations, the pressure is almost constant along the pipe. The temperature remains constant in the lower section of the tube also. Its amplitude experiences a sudden jump on crossing the source, followed by a rapid decay due to mixing with the unheated air.

The density variation shows that air expands after passing through the heat source. The similar but inverted functional form exhibited by the density may be anticipated from the ideal gas equation. Results provide numerical predictions for local flow properties, especially, at both ends of the heat source. Such information may be useful in setting up a semi-analytical model that leads to the asymptotic determination of p', u', and q'.

D. Relocating the Source

The location of the source is a key factor in producing large amplitude oscillations. When the

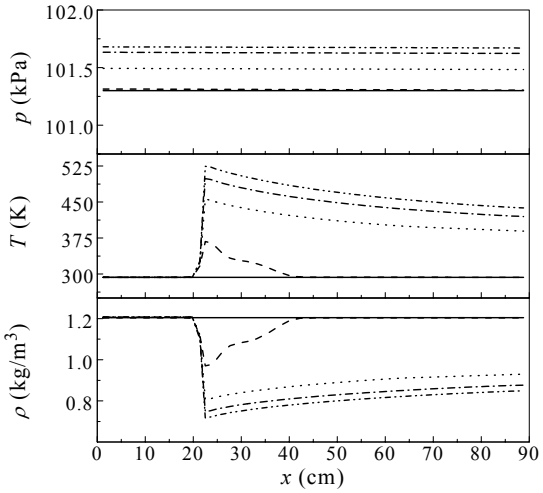

Fig. 7 Spatial distribution of steady pressure, temperature and density at several times before the inception of oscillations. Starting from rest, time evolutions are shown at finite steps corresponding to

$t =$ ——— 0; - - - - 2; ····· 4; -·-·-· 6; -···-··- 8 s.

source is placed in the lower half of the pipe, large amplitude oscillations are seen to occur. The resulting oscillations are found to have the largest amplitudes when the source is located at $(\frac{1}{4}l)$ from the bottom end. This is in accord with experimental findings reported previously.[1,4,5,7,16] During separate numerical runs, the source is relocated to the middle $(\frac{1}{2}l)$, and to the upper section $(\frac{2}{3}l)$ of the pipe in order to observe whether or not oscillations would occur.

Figures 8–9 are graphical representations of the pressure, axial velocity, temperature, density and source heat transfer versus time at the $\frac{1}{2}l$ and $\frac{2}{3}l$ heater locations. Results indicate that, when the source is positioned at $\frac{1}{2}l$, no oscillations are seen. The same can be said when the source is at $\frac{2}{3}l$. It is observed that oscillations occur only in the regions where acoustic velocity and pressure happen to have additive amplitudes (in the lower half of the tube). Maximum growth is noted where the modular product of acoustic pressure and velocity is maximized.

Figure 10 shows the temporal evolution of the source temperature T_{obs} at several locations. It can be observed that the heat source has a lower temperature when placed at $\frac{1}{4}l$ than at $\frac{1}{2}l$ and $\frac{2}{3}l$. This can be attributed to the larger transfer of energy to the acoustic waves when the source is located at $\frac{1}{4}l$ where heat conversion into acoustic energy is maximized. A

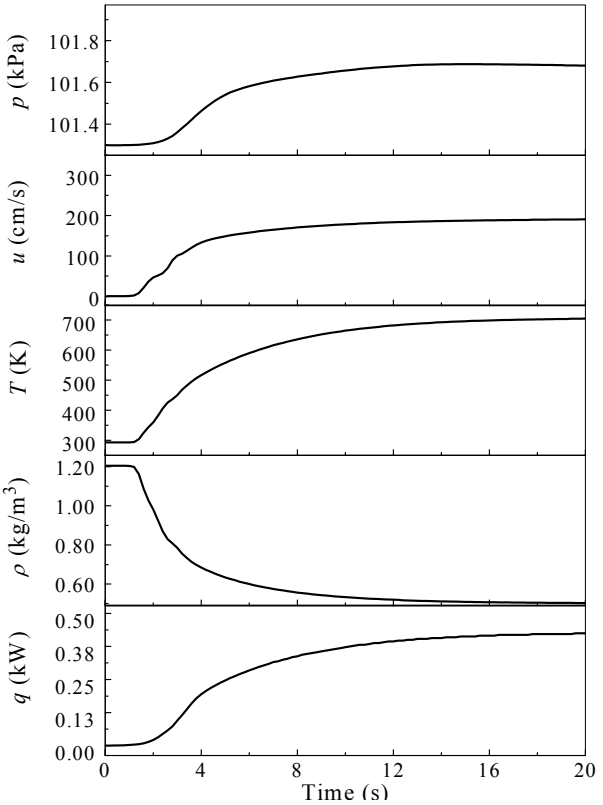

Fig. 8 Time evolution of pressure, axial velocity, temperature, density, and heat transfer during the first 20.0 seconds of the numerical simulations. Keeping the power input at the benchmark value of 430 watts, the heater is now moved to $x = \frac{1}{2}l$. Clearly, oscillations are suppressed when moving away from the optimal quarter length location.

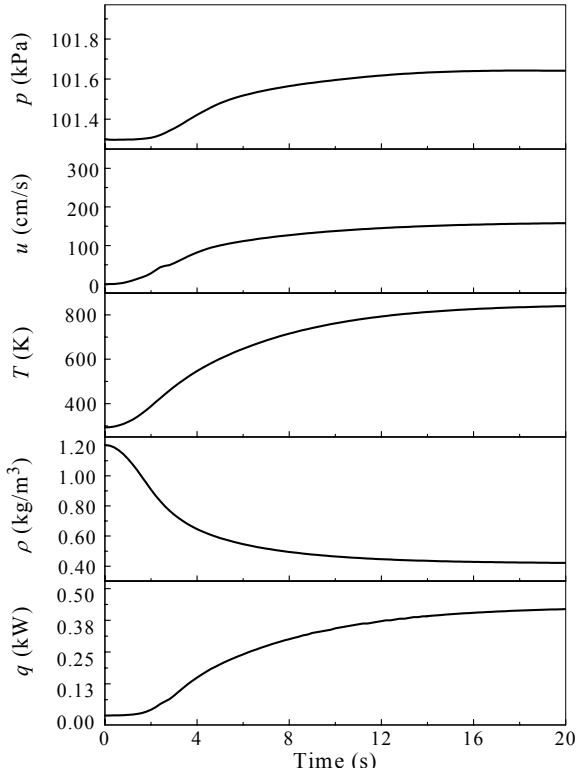

Fig. 9 Same as in the previous figure at the exception of the heat source being moved to $x = \frac{2}{3}l$.

similar thermal character has been reported in coal-fired gas turbines.[29,33]

E. Varying the Heat Power Input

While the standard conditions stated above are retained, the heat power input to the source is now varied. Keeping the source at the ideal $\frac{1}{4}l$ position, several heat power levels of 125.5, 376.6, 408.0, 426.9, 430.0, 433.1, and 439.4 watts are now released. The effect of varying the heat input on the induced acoustic motion can thus be captured.

Figure 11 is a graphical representation of the pressure for the first 20 seconds. For sufficiently small input (e.g., 125.5 W or below) no sign of oscillations can be seen. We infer that the heat input level, which feeds the acoustic oscillations, must possess some low threshold value. For the benchmark case chosen here, self-sustaining acoustic oscillations are established when the heat input exceeds a threshold value of 376 watts. Below this value, no appreciable acoustic oscillations can occur.

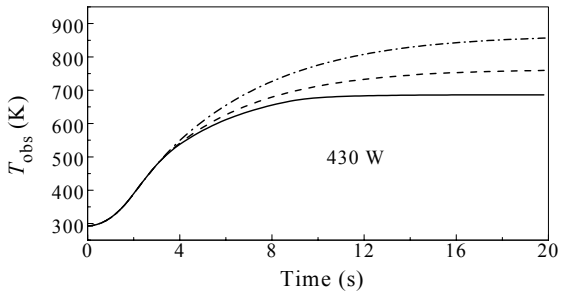

Fig. 10 Time evolution of the surface temperature for the heat source when located at $x = \frac{1}{4}l$ (——), $\frac{1}{2}l$ (- - -), and $\frac{2}{3}l$ (– – –).

Our experiments indicate the presence of another critical value beyond which the acoustic growth becomes very pronounced. This is illustrated is Fig. 12 where maximum pressure amplitudes are shown along with the sound pressure levels that accompany them. Clearly, large decibels are detected when the heat power input is in excess of 427 W. In fact, somewhere between 427 and 433 W, a sudden jump in the pressure output levels is observed with repeated runs. This

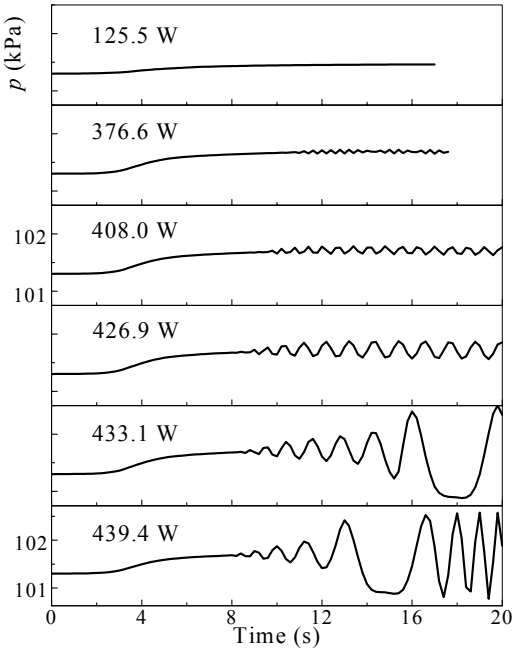

Fig. 11 Time evolution of pressure for different power inputs (Stage I). This a standard run with the heat source located at the optimal distance $x = \frac{1}{4}l$.

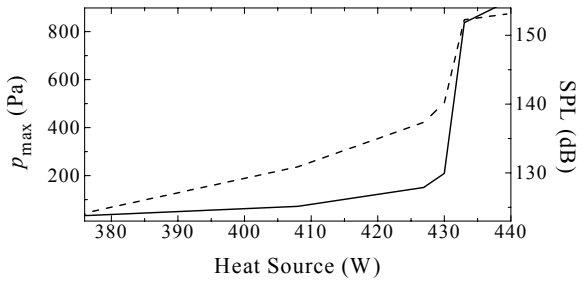

Fig. 12 Plot of maximum pressure (——) and corresponding sound pressure levels (- - -) for a range of heat power input levels at the source. Note the sudden pressure jump near a critical power input of approximately 430 W.

phenomenon is akin to resonance and is reproducible at a critical heat power input of approximately 430 W.

F. Acoustic Pressure and Velocity Mode Shapes

The acoustic pressure and velocity mode shapes obtained numerically are in general accord with one-dimensional, plane wave theory. As shown in Fig. 13, the oscillatory pressure reaches its maximum value at the center of the pipe and is a minimum near both ends. This mode shape concurs with classic theory. Likewise, acoustic velocity reaches its local maximum near both ends and is a minimum at the center of the pipe. This is also in agreement with acoustic theory. However, an interesting result can be seen in the velocity mode shape near the heater source. There, a local distortion (which is not predictable by simple plane wave theory) appears in the velocity amplitude. The increased local velocity can be ascribed to the strong coupling between velocity and thermal oscillations near the source. This condition is hoped to be later reproduced while constructing more elaborate analytical models.

G. Acoustic Phase Angles

Figure 14 shows the relationship between pressure, velocity and heat transfer oscillations at the source location. In conformance with acoustic theory, the pressure leads the velocity oscillation by a 90° phase angle. Interestingly, we find that q' is leading u' by 45°, and lagging p' by the same amount. In a former study, Carvalho[4] had demonstrated that the phase between acoustic pressure and heat had to be less than 90°. His hypothesis is in agreement with our result which suggests a phase lag of 45°. In supplementing Carvalho's analytical model, we now propose that a

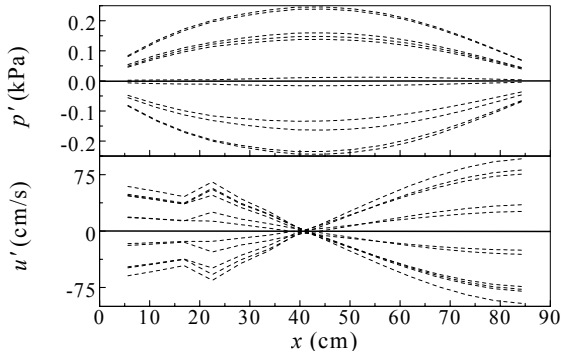

Fig. 13 Plot of acoustic pressure and velocity versus distance for several discrete times in a cycle.

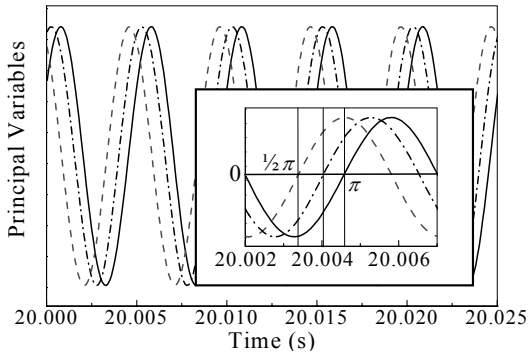

Fig. 14 Relationship between temporal pressure (——), axial velocity (- - -), and heat flux (– – –) at the optimal $x = \frac{1}{4}l$ location. Results are shown during the limit-cycle oscillations of Stage II.

value of $\phi = \pi / 4$ may be used in his expression for pressure oscillations. Repeated here for convenience, the pertinent equation reads

$$p' = A \sin \frac{m\pi x}{l} \sin\left(\omega t + \phi\right) \tag{3}$$

where ϕ is the phase lead between p' and q'. In the former article[4] this term was left unspecified.

H. The Thermoacoustic Form of Coupling

Suspecting a relationship between thermal and mechanical energy (in the form acoustic intensity, $p'u'$), we have decided to plot the modulus of heat oscillations alongside the modulus of the acoustic intensity. Based on our numerical simulations, the modulus of the heat transfer oscillation q' appears to be proportional to the modular product of acoustic velocity and pressures $p'u'$. As shown in Fig. 15, there is a strong indication of an intimate coupling between q' and $p'u'$ in the standing wave field. Physically, these observations suggest that a direct conversion of heat into mechanical energy may exist. A simple expression for q' may be proposed. Since the heat at the source is produced per unit area, and for dimensional homogeneity, the constant cross-sectional flow area may be factored in. Thus one may write

$$| q' | \sim | p'u' | A . \tag{4}$$

Equation (4) can be used in finding a solution to the set given by (1)–(2). This, it is hoped, will be demonstrated in a forthcoming article.

V. Conclusions

The numerical results described above, which agree with experimental observations, are supportive of a theory that attributes acoustic growth to the byproduct of pressure and velocity interactions. Both experimental observations and present numerical solutions agree that, unless the pressure and velocity have additive amplitudes, acoustic attenuation will prevail. This leads us to believe that velocity or pressure alone cannot be solely responsible for driving the oscillations. In fact, the main driving force may be ascribed to the thermal oscillations near the heat source. When thermal oscillations become self-sustained, acoustic pressure and velocity begin to grow in amplitude. When suitably added, they lead to a strong acoustic amplification and a relatively large conversion of thermal energy into sound. When the maximum amount of heat energy is converted into sound, the surface temperature at the source is minimized. Our study also suggests the presence of a minimum threshold value for the heat power supplied below which no self-sustained acoustic oscillations may be possible. In our numerical experiment, this value was 376 W. A critical value of the heat power input is also found to cause resonance to occur. When 430 W were supplied to the heater, a sharp peak in the acoustic amplitude was observed. The acoustic pressure and velocity mode shapes concur with classic theory throughout the tube. Near the heater, however, a marked increase is noted in the velocity amplitude that eludes plane wave acoustic theory. During limit-cycle oscillations, the acoustic pressure is found to lead thermal fluctuations by a 45 degree angle. The acoustic velocity also lags thermal fluctuations by the same amount. This numerically determined result helps complete Carvalho's solution. Finally, the modulus of heat oscillations is found, in all numerical experiments, to be proportional to the modulus of acoustic intensity.

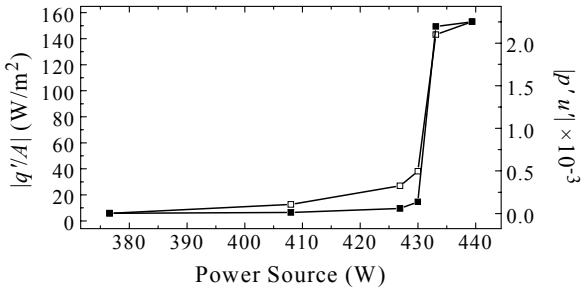

Fig. 15 Comparison between the modular product of acoustic pressure and velocity (–▫–), and the modulus of heat oscillation flux (–▪–).

References

[1]Bai, T., Cheng, X. C., Daniel, B. R., Jagoda, J. I., and Zinn, B. T., "Vortex Shedding and Periodic Combustion Processes in a Rijke Type Pulse Combustor," *Combustion Science & Technology,* Vol. 94, No. 1-6, 1993, pp. 245-258.

[2]Bai, T., Cheng, X. C., Daniel, B. R., Jagoda, J. I., and Zinn, B. T., "Performance of a Gas Burning Rijke Pulse Combustor with Tangential Reactants Injection," *Combustion Science & Technology,* Vol. 94, No. 1-6, 1993, pp. 1-10.

[3]Carrier, G. F., "The Mechanics of Rijke Tube," *Quarterly of Applied Mathematics,* Vol. 12, No. 4, 1955, pp. 383-395.

[4]Carvalho, J. A., Ferreira, C., Bressan, C., and Ferreira, G., "Definition of Heater Location to Drive Maximum Amplitude Acoustic Oscillations in a Rijke Tube," *Combustion and Flame,* Vol. 76, No. 1, 1989, pp. 17-27.

[5]Evans, R. E., and Putnam, A. A., "Rijke Tube Apparatus," *American Journal of Physics,* Vol. 34, 1966, pp. 360-361.

[6]Feldman, K. T., "Review of the Literature on Rijke Thermoacoustic Phenomena," *Journal of Sound and Vibration,* Vol. 7, 1968, pp. 83-89.

[7]Friedlander, M. M., Smith, T. J. B., and A, P., "Experiments on the Rijke Tube Phenomenon," *Journal of the Acoustical Society of America,* Vol. 36, 1964, pp. 1737-1738.

[8]Maling, G. C., "Simplified Analysis of the Rijke Phenomenon," *Journal of the Acoustical Society of America,* Vol. 35, 1963, pp. 1058-1060.

[9]Miller, J., and Carvalho, J. A., "Comments on Rijke Tube," *Scientific American,* Vol. 204, No. 3, 1961, pp. 180-182.

[10]Miller, N., Powell, E. A., Chen, F., and Zinn, B. T., "Use of Air Staging to Reduce the Nox Emissions from Coal Burning Rijke Pulse Combustors," *Combustion Science & Technology,* Vol. 94, No. 1-6, 1993, pp. 411-426.

[11]Raun, R. L., Beckstead, M. W., Finlinson, J. C., and Brooks, K. P., "Review of Rijke Tubes, Rijke Burners and Related Devices," *Progress in Energy & Combustion Science,* Vol. 19, No. 4, 1993, pp. 313-364.

[12]Raun, R. L., and Beckstead, M. W., "Numerical Model for Temperature Gradient and Particle Effects on Rijke Burner Oscillations," *Combustion & Flame,* Vol. 94, No. 1-2, 1993, pp. 1-24.

[13]Wang, M.-R., and Zinn, B. T., "Controlling Processes in Rijke Type Coal Burning Pulsating Combustors," *Chemical and Physical Processes in Combustion,* Vol. 61, 1984, pp. 1-61.

[14]Wang, M.-R., and Zinn, B. T., "Performance Characteristics of a Prototype, Rijke Type Pulsating Combustor," *Journal of the Chinese Society of Mechanical Engineers,* Vol. 8, No. 5, 1987, pp. 339-345.

[15]Xu, Z. X., Reiner, D., Su, A., Bai, T., Daniel, B. R. *et al.*, "Flame Stabilization and Combustion of Heavy Liquid Fuels in a Rijke Type Pulse Combustor," Fossil Fuel Combustion, ASME, Petroleum Division Paper PD 33, 1991.

[16]Zinn, B. T., Miller, N., A, C. J., and R, D. B., "Pulsating Combustion of Coal in a Rijke Type Combustor," Proceedings of the 19th International Symposium on Combustion,, 1982.

[17]Zinn, B. T., "State of the Art Research Needs of Pulsating Combustion," Noise Control & Acoustics, ASME Paper 84-WA NCA-19, 1984.

[18]Zinn, B. T., "Pulse Combustion: Recent Applications and Research Issues," Proceedings of the 24th International Symposium On Combustion, Combustion Institute Paper 19626, 1992.

[19]Kinsler, L. E., Frey, A. R., Coppens, A. B., and Sanders, J. V., *Fundamentals of Acoustics*, John Wiley, New York, 1982.

[20]Rayleigh, J. W. S., *The Theory of Sound*, Vol. 1-2, Dover Publications, New York, 1945.

[21]Bistafa, S. R., Lauchle, G. C., and Reethof, G., "Noise Generated by Cavitation in Orifice Plates," *Journal of Fluids Engineering-Transactions of the ASME,* Vol. 111, No. 3, 1989, pp. 278-289.

[22]Chen, T. Y., Hegde, U. G., Daniel, B. R., and Zinn, B. T., "Flame Radiation and Acoustic Intensity Measurements in Acoustically Excited Diffusion Flames," *Journal of Propulsion & Power,* Vol. 9, No. 2, 1993, pp. 210-216.

[23]Dowling, A. P., and Efows Williams, J. E., *Sound and Source of Sound*, Ellis Horwood, West Sussex, England, 1983.

[24]Hegde, U. G., Reuter, D., and Zinn, B. T., "Sound Generation by Ducted Flames," *AIAA Journal,* Vol. 26, No. 5, 1988, pp. 532-537.

[25]Ku, S. H., Cheng, S. C., Daniel, B. R., Jagoda, J. I., and Zinn, B. T., "Driving Processes in Gas Fired Pulse Combustors," *Chemical and Physical Processes in Combustion,* Vol. 84, No. 4, 1986, pp. 1-84.

[26]Lieuwen, T., and Zinn, B. T., "Role of Equivalence Ratio Oscillations in Driving Combustion Instabilities in Low Nox Gas Turbines," *Symposium (International) on Combustion,* Vol. 2, 1998, pp. 1809-1816.

[27]Neumeir, Y., Jagoda, J. I., and Zinn, B. T., "Modelling of Pulse Combustor Flapper Valves," *Fossil Fuel Combustion,* Vol. 33, 1991, pp. 117-125.

[28]Oran, E. S., and Gardner, J. H., "Chemical Acoustic Interactions in Combustion Systems," *Progress in Energy and Combustion Science,* Vol. 11, No. 4, 1985, pp. 253-276.

[29]Richards, G. A., Morris, G. J., Shaw, D. W., Keeley, S. A., and Welter, M. J., "Thermal Pulse Combustion," *Combustion Science & Technology,* Vol. 94, No. 16, 1993, pp. 57-85.

[30]Yavuzkurt, S., Ha, M. Y., Reethof, G., Koopmann, G., and Scaroni, A. W., "Effect of an Acoustic Field on the Combustion of Coal Particles in a Flat Flame Burner," *Journal of Energy Resources Technology-Transactions of the ASME,* Vol. 113, No. 4, 1991, pp. 286-293.

[31]Chu, B.-T., "Stability of Systems Containing a Heat Source -the Rayleigh Criterion," Research Memorandum Rept. 56D27, NACA, 1956.

[32]Flow-3D, Flow-Science Incorporated, Los Alamos, New Mexico, 1997.

[33]Richards, G. A., Logan, R. G., Meyer, C. T., and Anderson, R. J., "Ash Deposition at Coal-Fired Gas Turbine Conditions: Surface and Combustion Temperature Effects," *Journal of Engineering for Gas Turbines & Power-Transactions of the ASME,* Vol. 114, No. 1, 1992, pp. 132-138.